Aalborg Universitet

AALBORG UNIVERSITY

A Dual-Band Shared-Aperture Antenna with Wide-Angle Scanning Capability for Mobile System Applications

Yang, Guangwei; Zhang, Shuai

Published in:
I E E E Transactions on Vehicular Technology

DOI (link to publication from Publisher):
10.1109/TVT.2021.3072556

Creative Commons License
Unspecified

Publication date:
2021

Document Version
Accepted author manuscript, peer reviewed version

Link to publication from Aalborg University

Citation for published version (APA):
Yang, G., & Zhang, S. (2021). A Dual-Band Shared-Aperture Antenna with Wide-Angle Scanning Capability for Mobile System Applications. *I E E E Transactions on Vehicular Technology*, *70*(5), 4088-4097. Article 9400754. https://doi.org/10.1109/TVT.2021.3072556

General rights
Copyright and moral rights for the publications made accessible in the public portal are retained by the authors and/or other copyright owners and it is a condition of accessing publications that users recognise and abide by the legal requirements associated with these rights.

- Users may download and print one copy of any publication from the public portal for the purpose of private study or research.
- You may not further distribute the material or use it for any profit-making activity or commercial gain
- You may freely distribute the URL identifying the publication in the public portal -

Take down policy
If you believe that this document breaches copyright please contact us at vbn@aub.aau.dk providing details, and we will remove access to the work immediately and investigate your claim.

Downloaded from vbn.aau.dk on: December 06, 2025

A Dual-Band Shared-Aperture Antenna with Wide-Angle Scanning Capability for Mobile System Applications

Guangwei Yang, *Member, IEEE*, and Shuai Zhang, *Senior Member, IEEE*

***Abstract*—A dual-band shared-aperture phased array antenna with wide-angle scanning capability (WASC) is presented in this paper for mobile communications. Each shared-aperture antenna element consists of two wideband microstrip antenna units with air-cavity for the *C*-band and one wide beam magnetic-electro dipole antenna unit for the *S*-band. To achieve the wide-angle scanning, a phased array should have low inter-element mutual coupling and wide array-element beam-width. A simple metallic strip (MS), comprising four metal stubs and one rectangle shaped metal pillar, is utilized to improve the inter-element isolation of the array in and between the *C*- and *S*-bands. Furthermore, the metal strip can also broaden the beam-width of the *C*-band antenna units without distorting the wide-beam property of the *S*-band units. The shared-aperture array with a simple metallic strip is designed based on the above elements, and WASC is realized in both the *C*- and *S*- bands with low mutual coupling. To verify the proposed method, the shared-aperture array is fabricated and characterized, yielding good performance within the overall operating bandwidth. The measured results align very well with the simulated. The proposed array realizes the scanning coverage of ±60° with realized gain reduction of less than 3dB in both the *C*- and *S*-bands, which is a good candidate for the base station in the mobile environment.**

***Index Terms*—phased array, wide-angle scanning, scanning antennas, shared-aperture antennas, mobile communication, beamforming.**

I. Introduction

RECENTLY, with ever-increasing demand for wireless communication, 5G communication system has been widely applied because of large system capacity and high spectrum efficiency [1], especially in mobile communication system. The intelligent transportation system (ITS) is more and more popular in recent years, where supports various applications including autonomous vehicle operation, smart vehicular system, in-car delivery of infotainment services and safe driving assistance system [2]. Its communication methods consist of the vehicle to vehicle, base station to vehicle, base station to unmanned aerial vehicle (UAV) and vehicle to UAV [3] [4], and so on. To satisfy the communication system of ITS, various antennas [5]-[12] have been designed and applied. However, to ensure large date rate for ITS, the 5G communication system plays a pivotal role, which can improve the system capacity, transmission scope, and spectrum efficiency [13] [14]. Hence, some smart antennas come in as right candidates aimed to ensure high-speed mobile communication. Beam-steering technology is a good method to realize high-performance communication, as depicted in Fig. 1, which scans the beam to the high-speed targets and nulls to the interference, simultaneously. Therefore, the wide-angle scanning array antenna has become a hotspot, and the main topic for global researchers and scholars [15]-[22]. To realize wide-angle scanning capability (WASC) for array antennas, at present, the following methods are adopted. One is broadening the beam-width of the array element through designing the tapered slot [15], utilizing metal cavity [16], adding metal walls [17], and artificial magnetic conductor (AMC) [18], and so on. Another one is decoupling technology, where is realized by defected ground structure (DGS) [19], polarization-conversion isolator (PCS) [20], high impedance surface (HIS) [21], decoupling network [22], Metamaterials and metasurface[23], and so on[24][25]. Besides, some frequency scanning antennas [26]-[28] also realize wide-angle scanning capability, but which is different technology with the above literature.

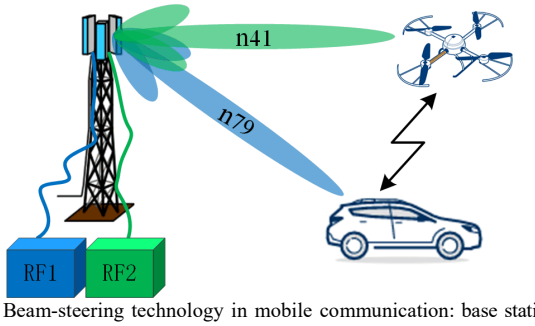

Fig. 1. Beam-steering technology in mobile communication: base station to vehicle and base station to UAV.

In modern communication systems, in order to cope with the complex communication environment, multi-band system is a

Manuscript received Dec. 22, 2020. This work has been supported by AAU Young Talent Program and the UK Royal Society Newton International Fellowship under Grant NIF/R1/191365. (Corresponding author: *Shuai Zhang*)

The authors are with the Antennas, Propagation and Millimeter-Wave Systems Section, Department of Electronic Systems, Aalborg University, 9220 Aalborg, Denmark. (E-mail gwyang086@gmail.com; sz@es,aau.dk).

Guangwei Yang is also with the School of Electronic Engineering and Computer Science, Queen Mary University of London, London E1 4NS, UK.

good solution, which not only improves the above problem but also extends the system capacity and save space. In addition, it can also communicate with different frequency bands according to different communication targets and environments, as shown in Fig. 1. It is highly preferred that phased arrays can own large scan angle, and also operate in several frequency bands. Some dual-band wide-angle scanning phased arrays [30]-[32] have been designed to solve this issue. In [30], a slot-loaded antenna element is designed to realize a dual-band phased array with WASC. In [31], a reconfigurable frequency antenna element is applied to achieve a dual-band phased array with WASC. A differentially fed slot antenna element is designed to realize achieve a dual-band phased array with WASC [32]. However, the above scanning antennas are difficult to achieve multiple bands with a large frequency ratio and WASC due to the limitation of the array inter-element distance.

Tightly coupled/connected arrays can achieve wideband and WASC simultaneously [33]. However, in some applications, especially 5G massive MIMO, different bands are required to operate independently and with low inter-element mutual coupling. Besides, as shown in Fig.1, in industry phased arrays/massive MIMO arrays for different bands typically have different RF chains (including modules, chips, and so on), so it is very necessary to have independent ports for different bands than the combined ports of the wideband. Hence, tightly coupled/connected arrays are not suitable for this application.

Shared-aperture phased array antennas with WASC are promising candidates to solve the afore-mentioned problems. A shared-aperture antenna refers to a method in which multiple antennas with different functions share the same aperture. Compared with traditional antennas, shared-aperture antennas could save space which is the most remarkable feature [34]. In recent years, different types of shared-aperture antennas with scanning capability have been designed [35]-[38]: the metal shielding vias and defected ground structure are applied to suppress the coupling and eliminate the scanning blindness in the Ku/Ka-bands shared aperture antenna array to realize wide-angle scanning capability [35]. A radiating element based on coaxial printed rings is applied and integrated with multicore monolithic microwave integrated circuits to realize beam scanning performance [36]. The substrate-integrated waveguide (SIW) technology is used in [37] to design a compact structure for a shared-aperture antenna array with beam-scanning capability. In [38], a metamaterial-based stacked mushroom structure is designed to realize a low profile shared-aperture array antenna with wide-angle scanning capability. Various technologies have been applied to solve this issue. However, the WASC, bandwidth or inter-element isolation of the previous designs should be much further improved, especially in scanning gain fluctuation.

In this work, a dual-band shared-aperture phased array antenna (SAPA) with WASC is designed and presented for 5G NR band-n41(2469-2690MHz) in S-band and -n79(4400-5000GHz) in C-band in mobile communication systems. Each dual-band antenna element is composed of two wideband microstrip antenna units with air-cavity operating in the C-band and one wide beam magnetic-electro (ME) dipole antenna in the S-band. Two C-band units are placed upon two dipole plates of the S-band unit, respectively, to satisfy the array inter-element distances for the WASC in two frequency bands. A simple metallic strip is designed and applied in the array, which not only improves the port isolation in and between the C-and S- bands, but broadens the beam-width of the C-band unit without distorting the wide-beam of the *S*-band units. The designed shared-aperture array covers the bandwidth of 9.3% and 26.9% with high inter-element isolation of 18 dB and 20 dB in the S-band and C-band, respectively. The array can achieve a wide scanning angle of ±60° with the low gain fluctuation of 3 dB in both the bands. The array antenna design in this paper is able to achieve wide angle scanning capability in a relatively wide bandwidth and the gain fluctuation is better than most common aperture antennas in the scanning range. However, these advantages are achieved at the expense of the height of the proposed array antenna. Hence, the proposed array antenna is a good candidate for base stations of mobile communication systems.

The paper is organized as follows: In Section II, the shared-aperture antenna element and array are designed. The mechanism of the metallic strip is analyzed. The WASC of the proposed array is analyzed and the performance is demonstrated in Section III. The proposed array antenna is fabricated and measured in Section IV, where the comparison with the previously published works is also carried out. The conclusions are provided in Section V.

II. The Design Processing and Principle Analysis

A. *Shared-aperture antenna element design*

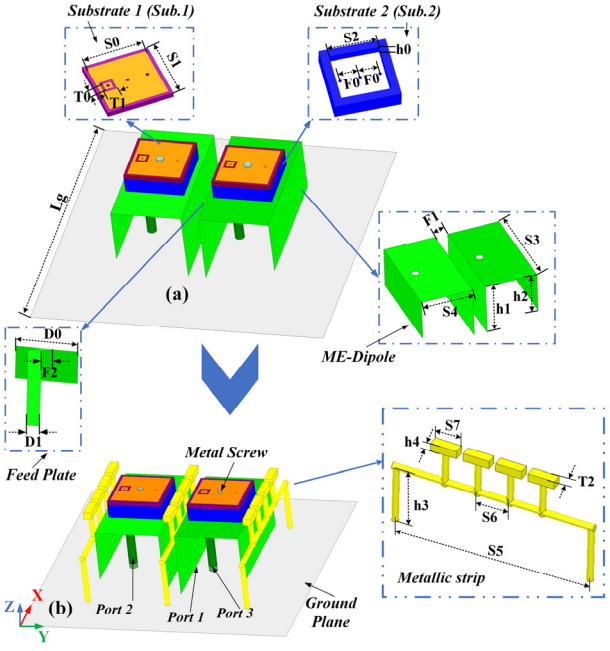

Fig. 2. Three-dimensional exploded view and design steps of the shared-aperture antenna element: (a) Referenced shared-aperture antenna (Ref.-SAPA); (b)the proposed antenna (Pro.-SAPA).

As the first step, it is necessary that designing suitable low and high band antenna units to satisfy the required inter-unit distance for both the low- and high-frequency bands according to the frequency ratio (1:2). As described in the Introduction, a dual-band shared-aperture antenna array with wide-angle scanning requires small inter-element distance, weak mutual coupling, and

broad element beam width in the respective frequency bands. The proposed two antenna elements (magnetic-electro (ME)-dipole element and air-cavity microstrip element) are also realize the capability of the wide beam with compact size. Besides, in the high0frequency band, a wide band antenna element is needed to cover the N79. Hence, the proposed configuration is designed and applied in the proposed system. And a good dual-band shared-aperture array with good wide-angle scanning capability is achieved, which is compared with the literature in [31][35]-[38]. As shown in Fig. 2, the three-dimensional exploded view and design steps of the proposed SAPA element are given. For the frequency bands of the application, an improved ME-dipole antenna [39] is applied as the *S*-band unit. And a substrate cavity microstrip antenna is designed to put the above on the plate of the ME-dipole antenna unit for the *C*-band unit. For the low-frequency band, it is good for wide-angle scanning capability that the proposed unit can radiate a wide beam pattern and make the structure compact, which consists of two bent metal plates, a U-shaped feed structure, and the ground plane. For the high-frequency band, a compact structure and wide-band antenna unit are needed, which should put on the limited ground plane (the plate of the ME-dipole unit) and mainly consists of three parts: a radiating patch on a thin substrate of Rogers RO4350B (with a relative dielectric constant of 3.66 and a loss tangent of 0.0027, and the thickness of 1.524mm) which is substrate 1 (Sub.1), a cavity substrate (which is the poly-tetra propylene with a relative dielectric constant of 2.2 and a loss tangent of 0.002) which is substrate 2 (Sub.2), and a metal probe. The key design parameters and stack diagram of the proposed shared-aperture antenna element are given in Fig. 2. All dimensions of the proposed antenna element, optimized by simulation, are shown in Table I. As we all know, the scanning coverage of the SAPA in two frequency bands would be larger with a smaller inter-element distance (even less than half wavelength) [40]. However, this can lead to a gain loss and strong inter-element mutual coupling. The strong coupling may distort the active VSWR when the array scans to a large angle, which limits the array scan angle. Moreover, the coupling among array elements could also affect the radiation patterns of the elements to even produce scan blindness [41]. Hence, the proposed antenna can't just combine two compact antenna units, the mutual coupling, extending the pattern, and port isolation between high and low bands in the array should be solved. As given in Fig. 2(b), a simple but useful structure is designed to improve the above problems to ensure a good WASC in the proposed SAPA.

TABLE I
OPTIMIZED DIMENSIONS OF THE PROPOSED ANTENNA ELEMENT (UNIT: MM)

Symbol	Lg	S_0	S_1	S_2	S_3	S_4	S_5	S_6	S_7	F_0	F_1
Value	50	18	20	15	45	24	60	10	6	6	6
Symbol	F_2	T_0	T_1	T_2	D_0	D_1	h_0	h_1	h_2	h_3	h_4
Value	4	2.5	4	3	14	3	2.5	24	19	18	2.0

For interpreting the function of the proposed structure, the E-field distribution of two type 1-by-2 antenna arrays is given in Fig. 3. In the S-band of 2469-2690MHz, as shown in Fig. 3(a), we can find that the microstrip patches (for C-band) on the driven unit can get a strong induced E-field when port1 is excited. And the coupling of the adjacent ME-dipole unit (port4 for S-band) is relatively weak. As given in Fig. 3(b), a metallic strip is applied in the array. It consists of four metal stubs and one rectangle-shaped metal pillar. It can be induced a strong E-field and weaken the E-field coupled to the microstrip patch. Besides, as a passive scatter, it also prevents a little E-field to couple the adjacent ME-dipole units. In the C-band of 4400-5000MHz, as shown in Fig. 3(c), when port 3 is excited, the E-field can be induced on the adjacent units by the spacing coupling. In the meanwhile, some E-field could be induced between the ground plane (the plate of the ME-dipole unit) by the bending vertical plate. Hence, the mutual coupling in the proposed array is strong. In Fig. 3(d), the E-field from the driven unit is mostly blocked by the metal strip to weaken the mutual coupling between the C-band patch units. Meanwhile, the proposed metallic strip also traps the coupling between the bending vertical plates. Hence, by comparing Fig. 3(c) and (d), we can find that the coupled E-field of the matching units is weakened due to the metallic strip.

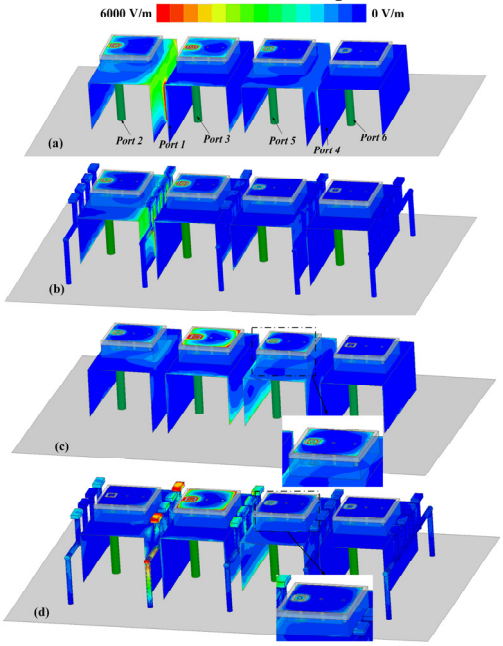

Fig.3. E-field distribution of Ref.-SAPA: (a) 2.7GHz; (c) 4.9GHz; and Pro.-SAPA:(b) 2.7GHz; (d) 4.9GHz.

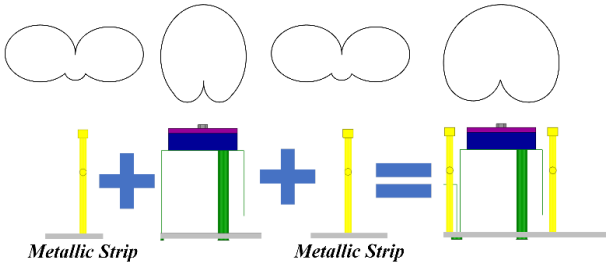

Fig. 4. The analysis of broadening the radiation pattern of high-frequency units

The proposed structure can also improve the beam-width of the C-band array units. According to the above mentioned, the

E-field can be induced on the metallic strip by the driven unit. So the vertical current is produced on the metallic strip. As reported in Fig. 4, the patch antenna can radiate a broadside-direction pattern, but which is narrow. The metallic strip can induce the E-filed from the patch antenna and radiate the pattern like the monopole. After combining the metallic strips and the patch antenna, the radiation pattern is broadened.

The simulated scattering parameters of two shared-aperture antennas are given in Fig. 5. For the Ref.-SAPA, as shown in Fig. 5(a), the impedance bandwidth (port1) of the ME-dipole unit in the S-band is from 2.55 to 2.80 GHz (9.3%). Although, the ME-dipole antenna is a wideband antenna. To reduce the interactions between *S*- and *C*-bands of the SAPA element and balance the radiation performance of the antenna, the ME-dipole antenna unit has to focus on the structure size reduction and wide-beam performance and ignores the wideband performance. The impedance bandwidth (port 2 or 3) of the substrate cavity patch unit at the *C*-band is from 4.40 to 6.15 GHz (33.2%). And the mutual coupling between port 2 and 3 is from -11 to -15dB in the frequency bands. The antenna unit has a wideband characteristic with a compact structure of about $\lambda/3$ (at 5.0 GHz). The port isolation in the *S*- and *C*-bands is just better than 12dB and 15dB, respectively. The radiation patterns in the *yoz*-plane are reported in Fig. 6. As the above said, the ME-dipole element can radiate a wide beam. However, for the *C*-band, two patch units can radiate different patterns which are narrow beam patterns, because of the asymmetrical ground plane (ME-dipole plate).

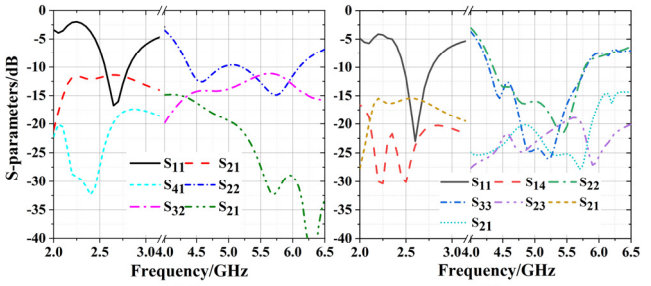

Fig. 5. Simulated S-parameters of two type of shared-aperture antennas: (a) without metallic strip; and (b) with metallic strip.

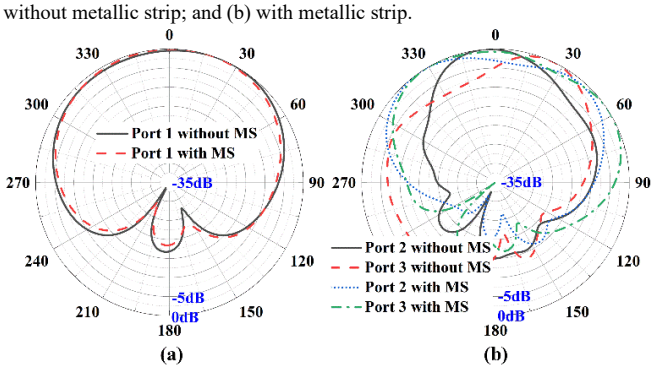

Fig. 6. Simulated radiation patterns in *yoz*-plane of two type shared-aperture antennas:(a) 2.7GHz; (b) 4.9GHz.

As the principle analysis mentioned, the metallic strip is applied to improve the above issues. As shown in Fig. 5(b), the S-parameters of the array are improved when the MS is added to the array. We can find that the operating bandwidth in the two bands is similar, but the port isolation between two low and high bands is improved. The mutual coupling is lower than -15 and -20dB in the S-band and C-band, respectively, indicating a good decoupling performance in the shared-aperture antenna array. Besides, as given in Fig. 6(b), the radiation pattern in the high-frequency band is improved obviously, which is a wide beam. We can find that the pattern of the antenna element without MS is narrow and its 3dB-beam-width is lower than 55°. However, the MS is applied in the antenna element, it can be observed that the pattern is obviously broadened and the 3-dB-beam-width is more than 120°.

B. Parameter study

As shown in Fig. 7, we select the height (h_4) and length (S_7) of the metal stub to analyze the function of the MS. In Fig. 7(a) and (b), it is observed that the height of the stub a very critical parameter. It not only affects coupling and reflection coefficient, but also plays a decisive role in beam broadening. For the length (S_7), as depicted in Fig. 7(c) and (d), it can be found that the reflection coefficient becomes worse and worse with increasing S_7. Meanwhile, the mutual coupling between the high-frequency units changes higher and higher. However, the beam-width of the high-frequency unit changes a little with the variation of S_7. Therefore, the beam-width and the mutual coupling in the *C*-band are improved by the MS, simultaneously. The simulated S-parameters of the shared-aperture antenna element with MS are given in Fig. 5(b). Compared with the S-parameters without MS in Fig. 5(a), the mutual coupling in the two frequency bands is optimized while the high-frequency radiation beam is broadened through the MS, but the wide beam characteristics in the *S*-band are not affected. Therefore, the proposed design meets the basic requirements of a wide-angle scanning array antenna.

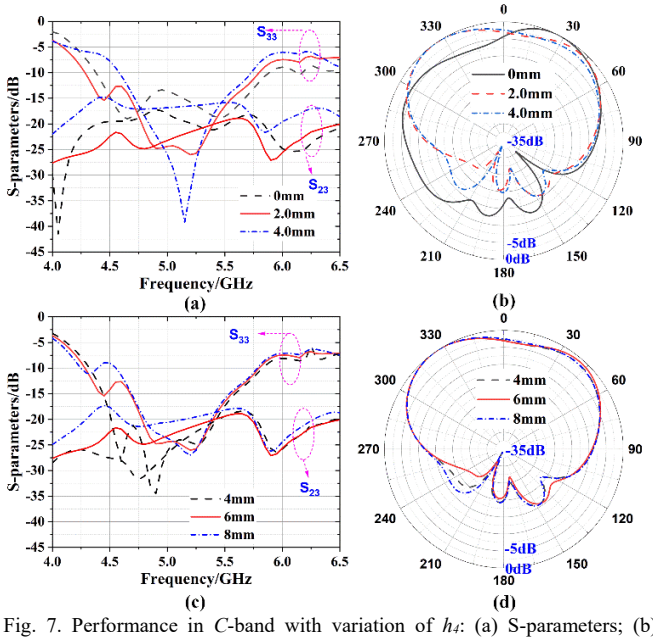

Fig. 7. Performance in *C*-band with variation of h_4: (a) S-parameters; (b) Radiation pattern of port 3; and S_7: (c) S-parameters; (d) Radiation pattern of port 3.

III. Performance Analysis of Shared-Aperture Array

A. SAPA with metallic strips

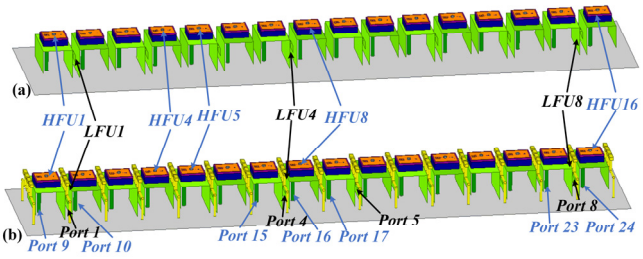

Fig. 8. The Geometry of the array antenna (low-frequency unit (LFU); High-frequency unit (HFU)).

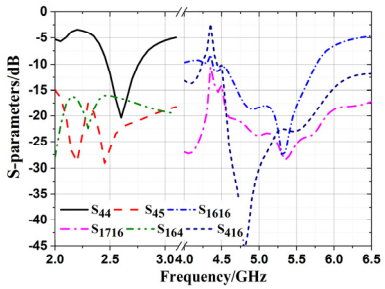

Fig. 9. Simulated S-parameters of the SAPA with metallic strip.

As depicted in Fig. 8, the shared-aperture array antenna with the metallic strip is designed. Thanks to the compact element size, the array consists of a 1×8 *S*-band linear array with the inter-unit distance of 60mm (0.56λ_l at 2.8GHz) and a 1×16 *C*-band linear array with the inter-unit distance of 30mm (0.55λ_h at 5.5GHz). The metallic strip is arranged between the high-frequency units in the array. The array ground plane has dimensions of 100mm×500mm. For this array antenna, the representative elements are selected to show the detailed scattering parameters in Fig. 9. The impedance bandwidth at the *C*-band is from 2.55 to 2.80 GHz (9.3%), within which the mutual coupling between the adjacent units is lower than -20dB in the above bandwidth. And the port isolation between low- and high-frequency ports is better than 16dB and consistent with one in Fig. 5(b). The impedance bandwidth in the *C*-band is from 4.4 to 5.85 GHz (28.3%), where the port isolation between the low- and high-frequency ports is better than 18dB. Furthermore, the mutual coupling between the *C*-band units is lower than -20 dB.

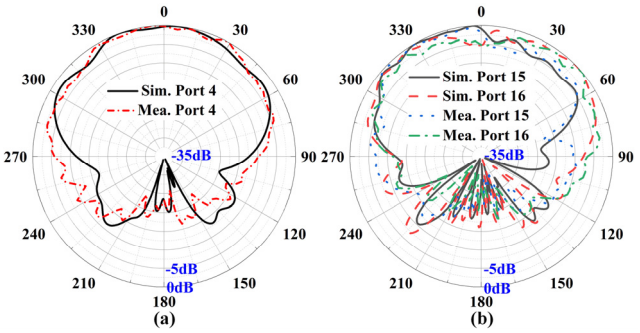

Fig. 10. The radiation patterns of the unit in the proposed array

To verify the broadening the beam-width capability of the metallic strip in the array, the radiation patterns of the center S-band and C-band units in the proposed array are shown in Fig. 10. It is observed that the radiation pattern in the S-band is still a wide beam pattern, which could ensure scanning larger coverage with a low gain loss. Similarly, for the C-band unit, the radiation patterns are also wide beam patterns, but it is asymmetric and the curve of the pattern has a little depression. This is because it has an asymmetric ground plane. Besides, the measured results of the patterns in the array also be given in this figure, we can find that the simulated and measured results are similar. In summary, the issues such as the mutual coupling and the port isolation of the SAPA, and the beam-width of the high-frequency unit are all solved because of the metallic strip which is a simple and effective structure. The SAPA with WASC would be realized in the proposed work, and the WASC will be analyzed and verified in the following parts.

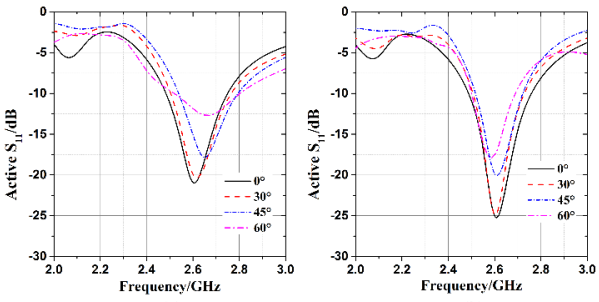

Fig. 11. Simulated active S_{11} in the S-band array with MS at different scanning angles: (a) LFU1; (b) LFU4.

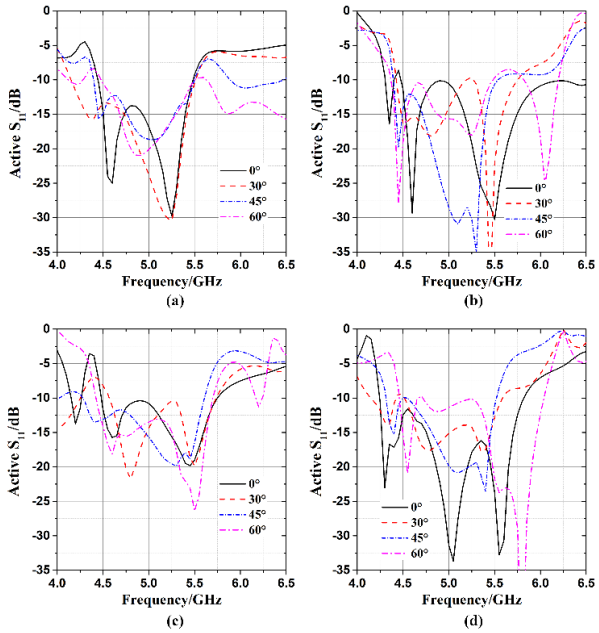

Fig. 12. Simulated active S_{11} in the C-band array with MS at different scanning angles: (a) HFU1; (b) HFU2; (c) HFU7; (d) HFU8.

B. *Simulated scanning performance analysis of the SAPA with metallic strip*

As described earlier, the improved SAPA has met the requirements of wide-angle scanning shared-aperture array antenna. Hence, we select some typical elements to report the scanning characteristics of the proposed array in Fig. 11 and Fig. 12. As shown in Fig. 11, the active S-parameters at 2.7 GHz with different scanning angles are given. The active S_{11} of two units is always lower than -10 dB in the bandwidth whatever the beam directs any angle in the coverage of ±60°. But the active S_{11} of LFU1 at 60° is not better than the one of LFU4. For the high-

frequency array, it is a 1×16 linear array, so the active S_{11} of four units in the array is shown in Fig. 12. It is observed that the active S_{11} is different with varying the scanning beam direction, but all of them are lower than -10dB in the frequency band. By analyzed the active S-parameters with varying the scanning beam direction, it is verified that the proposed SAPA with MS can achieve the WASC in two frequency bands with a large frequency ratio.

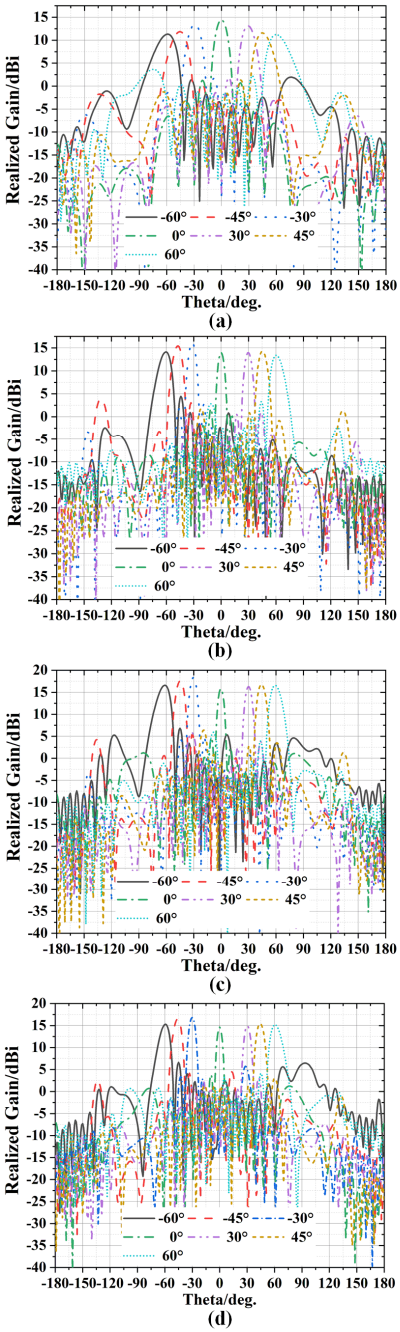

Fig. 13. Simulated scanning radiation patterns of SAPA with MS. (a) at 2.7GHz; (b) at 4.4GHz; (c) at 4.9GHz; (d)at 5.4GHz.

We select one frequency (2.7GHz) and three frequencies (4.4GHz, 4.9GHz, 5.4GHz) in the paper to analyze the radiation performance of two operating bands, respectively. As shown in Fig. 13 (a), for the WASC in the S-band, it can scan from -60° to 60°, and the realized gain drops with increasing scanning angles, but which's variation is less than 3dB. Meanwhile, the side-lobe level of every scanning pattern is less than -10dB. For the WASC of the proposed array in the *C*-band, the simulated scanning performance is depicted in Fig. 13 (b), (c), and (d). The patterns in the proposed operating band can scan the coverage of ±60° with the realized gain reduction of less than 3dB. For the realized gain of the scanning beam, it is different from the one in the S-band; the maximum gain is got at around -30°, not at broadside direction since the high-frequency units have an asymmetrical antenna structure. The SLL of every scanning beam is low than -10dB in all the scanning coverage.

By the above analysis, an ingenious structural design is presented, which realizes the shared-aperture array antenna with a frequency ratio of 2:1. However, to satisfy the WASC, a simple and effective structure is applied to improve the S-parameters of the proposed share-aperture antenna, meanwhile the wide-angle scanning impedance of the S- and C-bands is optimized, respectively. And the beam-width of the high-frequency unit in the array is extended. For verifying the proposed design method, the detailed scanning characteristics are analyzed and investigated in the following section.

IV. Experimental Results and Discussions

A. *Measurement setups*

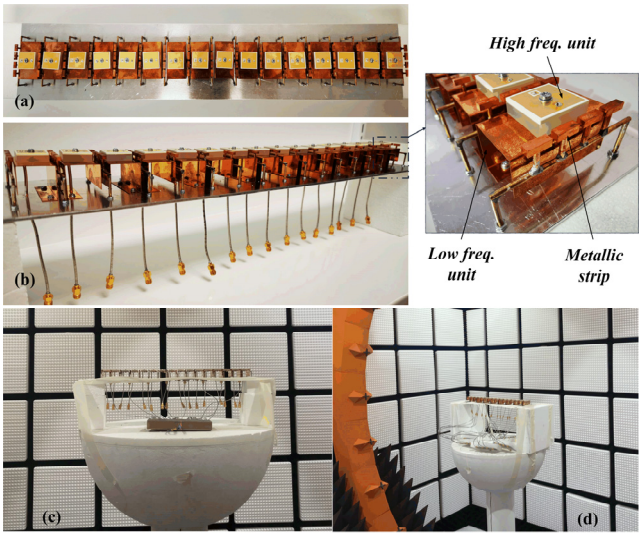

Fig. 14. The SAPA prototype and measurement process: (a) the top view of the array; (b) the array prototype; (c)the measured process in S-band; (d) the measured process in C-band.

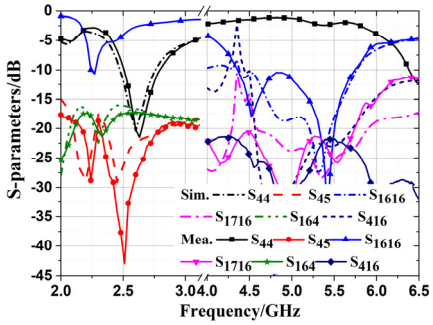

Fig. 15. Measured and simulated S-parameters of the SAPA with MS.

The dual-band shared-aperture wide-angle scanning array

antenna with MS is fabricated according to the previous design requirements, and validated in the SATIMO near-field measurement system, depicted in Fig. 14. The S-band units are made of copper with a thickness of 0.3mm. And the high-frequency units are fixed on the bent plate by the metal screws. Other parts of the array are fabricated as the design requirements. For measuring the proposed shared-aperture array antenna, the equal length cables, phase shifters, and power dividers are applied to ensure good experiment results. When the scanning performance at the low-frequency band is measured, the high-frequency units connect the terminal load, and vice versa.

B. The results analysis

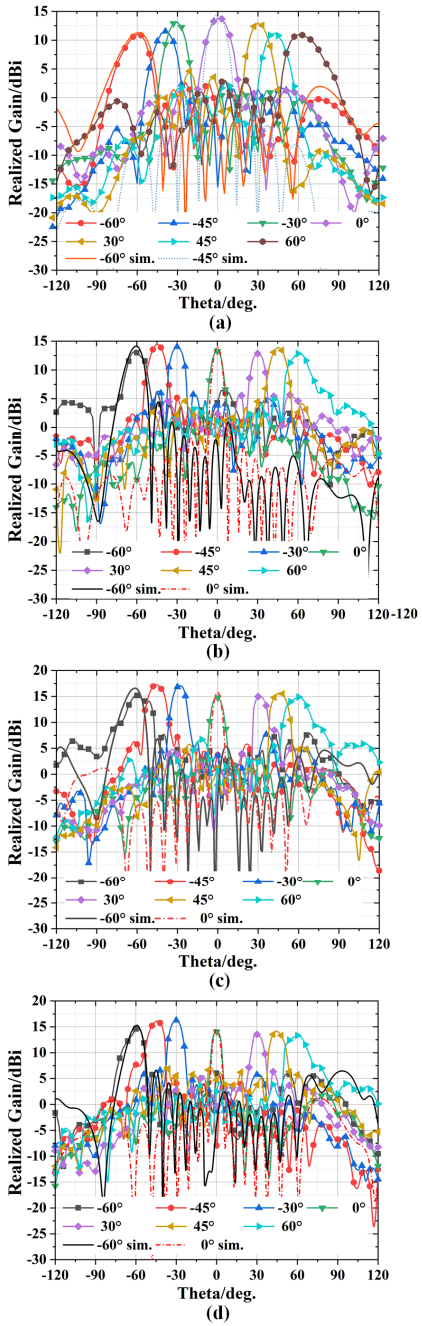

Fig. 16. Measured scanning radiation patterns of SAPA with MS. (a) at 2.7GHz; (b) at 4.4GHz; (c) at 4.9GHz; (d)at 5.4GHz.

The measured S-parameters of the SAPA with MS are shown in Fig. 15. From the figure, the measured results are very similar to the simulated results, especially in the S-band array. Since part of the antenna fabrication process is made manually, there are some differences between the measured and simulated S-parameters in the C-band, but it does not affect the antenna performance. For S-band array, the impedance bandwidth (≤-10dB) is from 2.5 to 2.8 GHz (9.3%), and the mutual coupling between elements in the array is lower than -20dB. The isolation port between low- and high-frequency units is better than 18dB. For the high-frequency array, the impedance bandwidth (≤-10dB) is a wide frequency band (26.9%) and from 4.35 to 5.7 GHz. For most of the operating band, the mutual coupling between the elements in the high-frequency array is lower than -20dB. The port isolation in the whole bandwidth is better than 22dB.

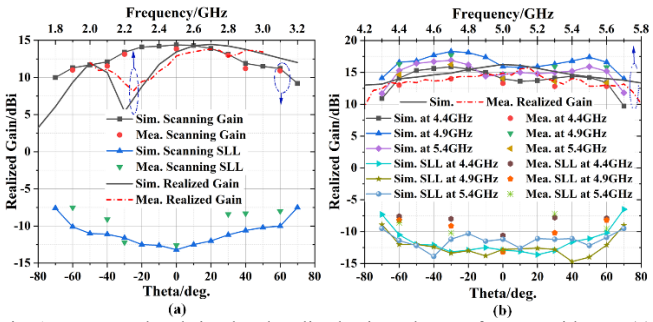

Fig. 17. Measured and simulated realized gain and SLL of SAPA with MS: (a) S-band; (b) C-band.

The measured scanning performance of the proposed shared-aperture array antenna is shown in Fig. 16. To analyze the simulated and measured results and demonstrate the WASC of the proposed shared-aperture array antenna, the detailed comparison is depicted in this figure. The measured results align very well with the simulated results, especially for the main-lobe, regardless of the scanning beam in any direction. However, the SLL and the realized gain has a little difference between the measured and simulated results, since there are fabrication errors and the alignment tolerance in assembly. Besides, the excitation amplitude obtained at each port is inconsistent due to the power splitter and the cable loss. The detailed radiation performance is given in Fig. 17. For the S-band, the measured and simulated realized gain in the operating band ranges from 12.9 to 13.8 dBi and from 13.4 to 14.5 dBi, respectively. And the scanning gain at 2.7GHz is from 11.4 to 14.4 dBi and from 10.9 to 13.8 dBi with the varying scanning coverage of ±60°. For *C*-band, the realized gain in the operating band is from 13.2 to 15.7 dBi for measurement, and from 14.0 to 16.2 dBi for simulation, respectively. At 4.4GHz, the measured realized gain varies from 12.8 to 14.0 dBi at the scan angle from -60° to 60°, the measured SLL is lower than -7.5dB. At 4.9GHz, it varies from 14.8 to 17.7 dBi in the scanning coverage. At 5.4 GHz, the measured gain variation is from 13.4 to 16.2 dBi with varying scanning angles. The SLL of these frequencies is lower than -7.3dB in the scanning coverage. Therefore, the WASC is applied to the shared-aperture phased array antenna to achieve the excellent dual-band shared-aperture

TABLE II
COMPARISON OF DIFFERENT DUAL-BAND ANTENNAS WITH WASC

Ref.	BW	Size(λ^3) (Element)	FR	SR	GF(dB)	SLL(dB)	PI(dB)	Efficiency
[31]	2.2% in L-band 3.4% in S-band	0.33×0.33×0.04	2.2:1	±60°	4dB in L/S-bands	-10	-23/-24	\
[35]	10.7% in Ku-band 9.1% in Ka-band	0.53×0.53×0.16	2:1	±45°	3dB in Ku-band 4.5dB in Ka-band	-21.2	\	58%/48.7%
[36]	4.9% in K-band 4.3% in Ka-band	0.37×0.40×2.14	1.5:1	±55°/±60°	7.5dB in K/Ka-bands	\	\	76%/73.4%
[37]	8.1% in Ku-band 5.5% in Ka-band	\	2.2:1	±40°	1.8dB in Ku/Ka-bands	-8.5/-8.0	-28/-70	\
[38]	11.7% in S-band 11.1% in X-band	0.18×0.18×0.02	2.7:1	±50°	5dB in S/X-bands	\	-10/-21	\
This work	**9.3% in S-band 26.9% in C-band**	**0.45×0.4×0.25**	**2:1**	**±60°**	**3dB in S/C-bands**	**-10**	**-18/-20**	**73.3%/68.2%**

BW: bandwidth; λ is the wavelength at the low frequency. FR: frequency ratio; SR: Scanning range; GF: the gain fluctuation in the scanning range; SLL: the side-lobe level; PI: the port isolation between dual bands.

antenna with wide-angle scanning capability.

C. Discussion

As described in Table II, compared the main performance of the proposed shared-aperture array with that of a typical sample for other published dual-band wide-angle scanning arrays. It is observed that the proposed dual-band array can realize excellent WASC and the scanning coverage of ±60° with the gain dropping of less than 3 dB in two bands with a large frequency ratio. In particular, the gain fluctuation is very low in the scan range of ±45°. Besides, the proposed antenna has a wide band especially in the high-frequency band and better port isolation. To the authors' best knowledge, this is the best dual-band shared-aperture array antenna with wide-angle scanning capability.

V. CONCLUSION

In this paper, a novel dual-band shared-aperture phased array antenna with WASC and frequency ratio of 2:1 is designed and applied in the mobile communication system. For the proposed scanning capability, two compact antenna units are designed, one is a wide beam ME-dipole antenna unit which has the size of 48×54×24mm^3, one is a wideband patch antenna unit which is put on the plate of the ME-dipole unit and has the size of 18 ×18×6mm^3. Besides, a simple metallic strip is used in the array to improve the inter-element mutual coupling of the proposed shared-aperture array, meanwhile, the isolation ports between S-and C-band units are improved, and more importantly, the radiation pattern of the high-frequency units is extended in the array. A shared-aperture array with the metallic strip is designed and fabricated to verify the proposed method, which's measured gain are from 12.9 to 13.8 dBi in the low-frequency band and from 13.2 to 15.7 dBi in the high-frequency band, respectively. The aperture efficiency of the proposed array is around 73.3% and 68.2% in the low- and high-frequency band, respectively. The proposed array can achieve the beam scanning up to ±60° with a realized gain reduction of less than 3.0 dB in the low operating band from 2.5 to 2.8 GHz and in the high operating band from 4.35 to 5.5 GHz, respectively. The measured results are similar to the simulated results and show the excellent wide-angle scanning capability of the shared-aperture phased array.

REFERENCES

[1] E. Telatar, "Capacity of multi-antenna Gaussian channels," *Eur. Trans. Telecommun.*, vol. 10, no. 6, pp. 585–595, Sep. 1999.

[2] T. E. Bogale, X. Wang and L. Le, "Adaptive Channel Prediction, Beamforming and Scheduling Design for 5G V2I Network: Analytical and Machine Learning Approaches," *IEEE Transactions on Vehicular Technology*, early access. 2020.

[3] M. Mozaffari, W. Saad, M. Bennis and M. Debbah, "Mobile Unmanned Aerial Vehicles (UAVs) for Energy-Efficient Internet of Things Communications," *IEEE Transactions on Wireless Communications*, vol. 16, no. 11, pp. 7574-7589, Nov. 2017.

[4] S. A. Hadiwardoyo, C. T. Calafate, J. Cano, Y. Ji, E. Hernández-Orallo and P. Manzoni, "3D Simulation Modeling of UAV-to-Car Communications," *IEEE Access*, vol. 7, pp. 8808-8823, 2019.

[5] H. Wong, K. K. So and X. Gao, "Bandwidth Enhancement of a Monopolar Patch Antenna With V-Shaped Slot for Car-to-Car and WLAN Communications," *IEEE Transactions on Vehicular Technology*, vol. 65, no. 3, pp. 1130-1136, March 2016.

[6] Q. Wu, Y. Zhou and S. Guo, "An L-Sleeve L-Monopole Antenna Fitting a Shark-Fin Module for Vehicular LTE, WLAN, and Car-to-Car Communications," *IEEE Transactions on Vehicular Technology*, vol. 67, no. 8, pp. 7170-7180, Aug. 2018.

[7] Z. Zhong et al., "A Compact Dual-Band Circularly Polarized Antenna with Wide Axial-Ratio Beamwidth for Vehicle GPS Satellite Navigation Application," *IEEE Transactions on Vehicular Technology*, vol. 68, no. 9, pp. 8683-8692, Sept. 2019.

[8] J. Zhu, Y. Yang, S. Li, S. Liao and Q. Xue, "Dual-Band Dual Circularly Polarized Antenna Array Using FSS-Integrated Polarization Rotation AMC Ground for Vehicle Satellite Communications," *IEEE Transactions on Vehicular Technology*, vol. 68, no. 11, pp. 10742-10751, Nov. 2019.

[9] C. Mao, S. Gao and Y. Wang, "Dual-Band Full-Duplex Tx/Rx Antennas for Vehicular Communications," *IEEE Transactions on Vehicular Technology*, vol. 67, no. 5, pp. 4059-4070, May 2018.

[10] L. Ge, S. Gao, Y. Li, W. Qin and J. Wang, "A Low-Profile Dual-Band Antenna with Different Polarization and Radiation Properties Over Two Bands for Vehicular Communications," *IEEE Transactions on Vehicular Technology*, vol. 68, no. 1, pp. 1004-1008, Jan. 2019.

[11] K. Min, S. Park, Y. Jang, T. Kim and S. Choi, "Antenna Ratio for Sum-Rate Maximization in Full-Duplex Large-Array Base Station with Half-Duplex Multiantenna Users," *IEEE Transactions on Vehicular Technology*, vol. 65, no. 12, pp. 10168-10173, Dec. 2016.

[12] Y. Han, W. Tang, S. Jin, C. Wen and X. Ma, "Large Intelligent Surface-Assisted Wireless Communication Exploiting Statistical CSI," *IEEE Transactions on Vehicular Technology*, vol. 68, no. 8, pp. 8238-8242, Aug. 2019.

[13] Z. MacHardy, A. Khan, K. Obana, and S. Iwashina, "V2X access technologies: Regulation, research, and remaining challenges," *IEEE Communications Surveys & Tutorials*, 2018.
[14] V. L. Nguyen, P. Lin and R. Hwang, "Enhancing misbehavior detection in 5G Vehicle-to-Vehicle communications," *IEEE Transactions on Vehicular Technology*, early access. 2020.
[15] A. Kedar and K. S. Beenamole. "Wide Beam Tapered Slot Antenna for Wide-angle Scanning Phased Array Antenna," Progress In Electromagnetics Research B, vol. 08, no. 1, pp. 235-251, 2011.
[16] Y. Q. Wen, B. Z. Wang, X. Ding, "Wide-Beam Siw-Slot Antenna for Wide-Angle Scanning Phased Array," *IEEE Antennas and Wireless Propagation Letters*, vol. 15, pp. 1638-1641, 2016.
[17] G. Yang, J. Li, S. G. Zhou, Y. Qi. "A Wide-Angle Scanning E-plane Linear Array Antenna with Wide Beam Elements," *IEEE Antennas Wireless Propag. Lett.*, vol. 16, pp. 2923–2926, Oct. 2017.
[18] R. Wang, B. Wang, X. Ding and X. Yang, "Planar Phased Array with Wide-Angle Scanning Performance Based on Image Theory," *IEEE Transactions on Antennas and Propagation*, vol. 63, no. 9, pp. 3908-3917, Sept. 2015.
[19] L. Gu, Y. W. Zhao, Q. M. Cai, Z. P. Zhang, B. H. Xu, Z. P. Nie, "Scanning Enhanced Low-profile Broadband Phased Array with Radiator-sharing Approach and Defected Ground Structures," *IEEE Transactions on Antennas and Propagation*, vol. 65, no. 11, pp. 5846-5854, Nov. 2017.
[20] Y. Cheng, X. Ding, G. Gao, W. Shao and C. Liao, "Analysis and Design of Wide-Scan Phased Array Using Polarization-Conversion Isolators," *IEEE Antenna and Wireless Propagation Letters*, vol. 18, no.3 pp. 512-516, Mar. 2019.
[21] G. Yang, J. Li, R. Xu, Y. M. Y. Qi, "Improving the Performance of Wide-Angle Scanning Antenna Array with High Impedance Periodic Structure," *IEEE Antennas Wireless Propag. Lett*., vol. 15, pp. 1819–1822, Mar. 2016.
[22] R. L. Xia, S. W. Qu, P. F. Li, D. Q. Yang, S. Yang, Z. P. Nie, "Wide-Angle Scanning Phased Array Using an Efficient Decoupling Network," *IEEE Transactions on Antennas and Propagation*, vol. 63, no. 11, pp. 5161-5165, Sep. 2015.
[23] M. Alibakhshikenari, F. Babaeian, Bal S. Virdee, et al., "A Comprehensive Survey on "Various Decoupling Mechanisms with Focus on Metamaterial and Metasurface Principles Applicable to SAR and MIMO Antenna Systems"," IEEE Access, vol. 8, pp. 192965-193004, 2020.
[24] Alibakhshikenari, Mohammad, Bal S. Virdee, and Ernesto Limiti. "Study on Isolation and Radiation Behaviours of a 34×34 Array-Antennas Based on SIW and Metasurface Properties for Applications in Terahertz Band Over 125-300 GHz", Optik, International Journal for Light and Electron Optics, Vol. 206, 163222, Mar. 2020.
[25] Alibakhshikenari M, Virdee B S, Shukla P, et al. "Isolation enhancement of densely packed array antennas with periodic MTM-photonic bandgap for SAR and MIMO systems," IET Microwaves, Antennas & Propagation, vol. 14, no. 3, pp. 183-188, Feb. 2019.
[26] M. Alibakhshikenari, Bal S. Virdee, Chan H. See, et al. "High-isolation leaky-wave array antenna based on CRLH-metamaterial implemented on SIW with±30º frequency beam-scanning capability at millimetre-waves," Electronics, vol. 8, no. 6, pp. 642, Jun. 2019.
[27] M. Alibakhshikenari, Bal S. Virdee, M. Khalily, et al. "Beam-scanning leaky-wave antenna based on CRLH-metamaterial for millimetre-wave applications," IET Microwaves, Antennas & Propagation, vol. 13, no. 8, pp. 1129-1133, Jul. 2019.
[28] M. Alibakhshikenari, Bal S. Virdee, A. Ali, et al. "A novel monofilar-Archimedean metamaterial inspired leaky-wave antenna for scanning application for passive radar systems," Microwave and Optical Technology Letters, vol. 60, no. 8, pp. 2055-2060, Jun. 2018.
[29] D. Wei, J. Li, J. Yang, Y. Qi and G. Yang, "Wide-Scanning-Angle Leaky-Wave Array Antenna Based on Microstrip SSPPs-TL," in IEEE Antennas and Wireless Propagation Letters, vol. 17, no. 8, pp. 1566-1570, Aug. 2018.
[30] S. E. Valavan, D. Tran, A. G. Yarovoy, A. G. Roederer, "Planar Dual-Band Wide-Scan Phased Array in X-Band," *IEEE Transactions on Antennas & Propagation*, vol. 62, no. 10, pp. 5370-5375, Oct. 2014.
[31] N. Haider, A. G. Yarovoy and A. G. Roederer, "L/S-Band Frequency Reconfigurable Multiscale Phased Array Antenna with Wide Angle Scanning," *IEEE Trans. Antennas Propag.*, vol. 65, no. 9, pp. 4519-4528, Sep. 2017.
[32] J. Guo, S. Xiao, S. Liao, B. Wang and Q. Xue, "Dual-Band and Low-Profile Differentially Fed Slot Antenna for Wide-Angle Scanning Phased Array," *IEEE Antennas and Wireless Propagation Letters*, vol. 17, no. 2, pp. 259-262, Feb. 2018.
[33] J. Zhong, A. Johnson, E. A. Alwan, J. L. Volakis, "Dual-linear polarized phased array with 9:1 bandwidth and 60° scanning off broadside", *IEEE Trans. Antennas Propag.*, vol. 67, no. 3, pp. 1996-2001, 2019.
[34] T. A. Axness, R. V. Coffman, B. A. Kopp, and K. W. O'Haver, "Shared aperture technology development, "John Hopkins APL Tech. Dig., vol. 17, no. 3, pp. 285–294, 1996
[35] S. Liu, K. Jiang, G. Xu, X. Ding, K. Zhang, J. Fu, Q. Wu, "A Dual-Band Shared Aperture Antenna Array in Ku/Ka-Bands for Beam Scanning Applications", *IEEE Access*, vol. 7, pp. 78794-78802, 2019.
[36] A. I. Sandhu, E. Arnieri, G. Amendola, L. Boccia, E. Meniconi and V. Ziegler, "Radiating elements for shared aperture Tx/Rx phased arrays at K/Ka band", *IEEE Trans. Antennas Propag.*, vol. 64, no. 6, pp. 2270-2282, Jun. 2016.
[37] Y. R. Ding and Y. J. Cheng, "Ku/Ka Dual-Band Dual-Polarized Shared-Aperture Beam-Scanning Antenna Array with High Isolation," *IEEE Transactions on Antennas and Propagation*, vol. 67, no. 4, pp. 2413-2422, April 2019.
[38] C. X. Bai, Y. J. Cheng, Y. R. Ding and J. F. Zhang, "A Metamaterial-Based S/X-Band Shared-Aperture Phased-Array Antenna with Wide Beam Scanning Coverage," *IEEE Transactions on Antennas and Propagation*, vol. 68, no. 6, pp. 4283-4292, June 2020.
[39] G. Yang, J. Li, J. Yang, S. G. Zhou. "A Wide Beam-width and Wideband Magnetoelectric Dipole Antenna," IEEE Transactions on Antennas and Propagation, vol. 66, no. 12, pp.6724-6733, Dec. 2018.
[40] N. Amitay, V. Galindo, and C. P. Wu, Theory and Analysis of Phased Array Antennas. New York, NY, USA: Wiley-Interscience, 1972.
[41] D.M. Pozar, "A relation between the active input impedance and the active element pattern of a phased array," *IEEE Transactions on Antennas and Propagation*, vol. 51, no. 9, pp. 2486-2489, Sep. 2003.